ISSN 1070-3284, Russian Journal of Coordination Chemistry, 2016, Vol. 42, No. 8, pp. 494–501. © Pleiades Publishing, Ltd., 2016.
Original Russian Text © I.A. Lutsenko, E.V. Korneeva, A.V. Ivanov, 2016, published in Koordinatsionnaya Khimiya, 2016, Vol. 42, No. 8, pp. 459–466.

Supramolecular Complexes $[M\{NH(CH_2)_4O\}\{S_2CN(C_2H_5)_2\}_2] \cdot CCl_4$ (M = Zn or ^{63}Cu(II)): Synthesis, Structures, Spectral and Thermal Properties

I. A. Lutsenko[a], *, E. V. Korneeva[b], and A. V. Ivanov[b]

[a] *Kurnakov Institute of General and Inorganic Chemistry, Russian Academy of Sciences, Leninskii pr. 31, Moscow, 119991 Russia*

[b] *Institute of Geology and Nature Management, Far East Branch, Russian Academy of Sciences, Blagoveshchensk, Russia*

**e-mail: irinalu05@rambler.ru*

Received December 8, 2015

Abstract—Solvated adducts of diethyldithiocarbamate complexes of zinc and copper(II) of the formula $[M\{NH(CH_2)_4O\}\{S_2CN(C_2H_5)_2\}_2] \cdot CCl_4$ (M = Zn (**I**) and ^{63}Cu (**II**)) were obtained. ^{13}C MAS NMR experiments revealed magnetic nonequivalence in the dithiocarbamate moieties of the adduct isomers, the morpholine heterocycles, and the outer-sphere solvate molecules. The rhombic anisotropy of the EPR parameters of magnetically diluted isotope-substituted complex **II** is due to the copper polyhedron geometry, which is intermediate between a tetragonal pyramid and a trigonal bipyramid, with the ground state of the unpaired electron resulting from the mixing of $3d_{x^2-y^2}$- and $3d_{z^2}$-AOs of copper(II). According to X-ray diffraction data, complex **I** is a supramolecular complex combining structurally nonequivalent adduct molecules (A and B) and "guest" molecules (CCl_4). In addition, the crystal lattice has an array of channels occupied by outer-sphere solvate CCl_4 molecules (a structural type of lattice clathrates). An STA study of the thermal properties revealed three main thermolysis steps: desorption of the solvate CCl_4 molecules, elimination of coordinated morpholine molecules, and thermolysis of the dithiocarbamate moiety of the adduct.

DOI: 10.1134/S1070328416080042

Coordinatively unsaturated dithiocarbamate complexes can reversibly add electron-donating organic bases [1–14]. Such adducts (complex + N-donating base) are of commercial interest because of their volatility *in vacuo*. Specifically, adduct formation and solvation of the resulting complexes enable (compared to the starting dialkyldithiocarbamates) a sequential shift of the thermal degradation range for the dithiocarbamate moiety to the lower temperatures [15]. The latter is useful in chemical vapor deposition of transition metal sulfides as thin films having semiconducting or luminescent properties [16].

Earlier, adducts of zinc(II) and copper(II) diethyldithiocarbamates with morpholine of the formula $[M\{NH(CH_2)_4O\}\{S_2CN(C_2H_5)_2\}_2]$ (M = Zn, ^{63}Cu, and ^{65}Cu) have been obtained preparatively [17–19]. According to the multinuclear (^{13}C, ^{15}N) MAS NMR, EPR, and X-ray diffraction data, these adducts exist in the crystal as two molecular forms exhibiting conformational isomerism. The conformers differ in M–N bond strength, metal polyhedron geometry ($[MNS_4]$), and the spatial orientation of the coordinated morpholine molecules. Solvation of these adducts with participation of the outer-sphere chlorohydrocarbon molecules in the system $[Zn_2\{S_2CN(C_2H_5)_2\}_4]$–$NH(CH_2)_4O$–L (L = CH_2Cl_2, $CHCl_3$, and 1,2-$C_2H_4Cl_2$) produces both various supramolecular complexes and new solvate molecules derived from morpholine and chlorohydrocarbons ($CH_2\{N(CH_2)_4O\}_2$, $C_2H_4\{N(CH_2)_4O\}_2$) [20–22].

The goal of this study was to obtain supramolecular complexes $[M\{NH(CH_2)_4O\}\{S_2CN(C_2H_5)_2\}_2] \cdot CCl_4$ (M = Zn (**I**) or ^{63}Cu (**II**)) and examine their structures, spectral and thermal properties by X-ray diffraction, EPR and ^{13}C MAS NMR spectroscopy, and simultaneous thermal analysis (STA).

EXPERIMENTAL

Synthesis of adduct I. The starting dinuclear zinc diethyldithiocarbamate complex, $[Zn_2(Edtc)_4]$, was obtained from $Na\{S_2CN(C_2H_5)_2\} \cdot 3H_2O$ (Sigma–Aldrich) and recrystallized as described in [23]. The complex $[Zn_2(Edtc)_4]$ (0.50 g, 0.69 mmol) was dissolved in CCl_4 (5 mL) upon slight heating (50°C). Morpholine (0.12 mL, 1.4 mmol; stoichiometric ratio 1 : 1) was added dropwise while stirring the resulting

solution. Slow evaporation of the solvent at 18°C gave crystals, which were separated from the mother liquor, dried in air, and stored in a sealed tube. The yield of adduct **I** was 69%.

Adduct II was synthesized in the isotope-substituted form as described for **I**. For this purpose, a copper(II) salt with a ^{63}Cu concentration of 99.3(1) at % was used. To enhance the resolution of EPR spectra, a sample of adduct **II** was magnetically diluted (Cu : Zn = 1 : 1000). The completeness of the conversion of the starting complex to the adduct was checked by gravimetry and EPR spectroscopy.

EPR spectra of magnetically diluted adduct **II** was recorded on a 70-02 XD/1 radio spectrometer (~9.5 GHz) at room temperature. The operating frequency was measured with a ChZ-46 microwave frequency meter. *g*-Factors were calculated with reference to DPPH. The error in the determination of *g*-factors was ±0.002; the hyperfine constants were determined with an accuracy of ±2%. EPR spectra were simulated in terms of second-order perturbation theory with the WIN-EPR SimFonia program (Bruker software, version 1.2). While fitting a simulated spectrum to the experimental one, *g*-factors, hyperfine constants, line widths, and percent contributions from the Lorentz and Gauss components to the line shapes were variables.

^{13}C MAS NMR spectra of adduct **I** were recorded on a CMX-360 spectrometer (Varian/Chemagnetics InfinityPlus) operating at 90.52 MHz (superconducting magnet with B_0 = 8.46 T; Fourier transform, 295 K). The ^{1}H–^{13}C cross polarization techniques were used; ^{13}C–^{1}H dipolar interactions were suppressed via proton decoupling in a magnetic field with the corresponding proton resonance frequency [24]. A sample (~350 mg) was packed into a zirconia rotor (7.5 mm in diameter). The spinning rates in ^{13}C MAS NMR experiments were 4500(2) Hz. The number of transients was 14400; the proton π/2-pulse length was 5.2 μs. The ^{1}H–^{13}C contact time was 2.0 ms; the pulse delays were 3.0 s. Isotropic ^{13}C chemical shifts δ (ppm) are referenced to a line of crystalline adamantane [25] used as an external standard (δ = 38.48 relative to tetramethylsilane [26]).

X-ray diffraction study of adduct I. Reflection intensities were measured at 293(2) K on a CAD-4 single-crystal four-circle diffractometer (CuK_α radiation, graphite monochromator, ω scan mode). The surface of a single-crystal sample was protected from degradation with an epoxy resin film. The unit cell parameters were determined and refined from 25 reflections for θ = 30°–37°. Primary processing of the experimental data was performed with the WinGX program package [27]. An absorption correction was applied upon the ω scanning [28] of five selected reflections. Structure **I** was solved by a direct method (SHELXS-97) [29] and refined anisotropically for all non-hydrogen atoms with the SHELXL-97 program [30]. The hydrogen atoms were located geometrically and refined together with their parent atoms using a riding model. In the refinement of structure **I**, Friedel pairs were not averaged; the absolute configuration was determined from the Flack parameter [30] found to be 0.00(4). The crystallographic parameters and data collection and refinement statistics for structure **I** are as follows: yellow needle-like crystals, 0.50 × 0.20 × 0.15 mm, monoclinic system, space group $P2_1$, a = 11.619(5), b = 8.690(2), c = 27.012(9) Å, β = 98.03(3)°, V = 2700.5(16) Å^3, Z = 4, ρ_{calcd} = 1.483 g/cm^3, μ = 7.898 mm^{-1}, θ = 1.65°–69.97°, ranges of h, k, l indices: $-12 \leqslant h \leqslant 14$, $-9 \leqslant k \leqslant 10$, $-32 \leqslant l \leqslant 32$, number of measured reflections 9629, number of unique reflections 8586, R_{int} = 0.0446, GOOF = 1.024, R_1 ($I > 2\sigma(I)$) = 0.0662, wR_2 ($I > 2\sigma(I)$) = 0.1694, T_{min}/T_{max} = 0.34/0.53, residual electron density (min/max) −0.646/0.637 e Å^{-3}. The atomic coordinates, bond lengths, and bond angles for structure **I** have been deposited with the Cambridge Structural Database (no. 968969; deposit@ccdc.cam.ac.uk or http://www.ccdc.cam.ac.uk).

The thermal behavior of adduct **I** was studied by the STA method combining TG and DSC measurements on an STA-449C Jupiter instrument (NETZSCH) in platinum crucibles. The cap of each crucible has an opening to provide a vapor pressure of 1 atm during thermolysis. Samples (4.57–4.70 mg) were heated under argon to 500°C at a heating rate of 5°C/min. The temperature measurement accuracy was ±0.7°C; weight measurements were accurate to within ±(1 × 10^{-4}) mg. TG and DSC curves were recorded using a correction file and temperature and sensitivity calibration data for a given temperature program and a given heating rate.

RESULTS AND DISCUSSION

The EPR spectrum of adduct **II** magnetically diluted with zinc is characterized by the rhombic anisotropy of the g- and A-tensors (Fig. 1*a*; Table 1). Each of the three orientations is manifested as a four-component hyperfine structure due to the ^{63}Cu nucleus (I = 3/2). (The previously recorded spectrum of the nonsolvated adduct (Table 1) corresponds to axial symmetry [18].) The high-field region contains two intense peaks due to additional absorption (AA) [31, 32]. Because the hyperfine lines associated with different orientations overlap the AA peaks, the calculated EPR parameters (Table 1) were refined by computer simulation. In a first step, we obtained first-derivative spectra. This was followed by taking the second derivatives of the experimental EPR spectra to make the hyperfine lines considerably narrower and enhance the resolution. In a second step, we strove to achieve as close an approximation as possible for the third derivatives of the simulated and experimental

spectra. The best-fit curve is shown in Fig. 1 (curve *b*); the corresponding parameters are given in Table 1.

The close similarity between the simulated and experimental spectra (Fig. 1) reflects fairly well the positions and relative intensities of the hyperfine lines for all the three orientations (including the positions of the AA peaks).

The observed rhombic anisotropy of the EPR parameters for complex **II** (Table 1) suggests a considerable rhombicity of the nearest environment of the metal center. For complexes of copper(II) with C.N. 5, this condition is met by polyhedra that have an intermediate geometry between tetragonal pyramid (TP) and trigonal bipyramid (TBP), and the ground state of the unpaired electron is produced by mixing the $3d_{x^2-y^2}$- and $3d_{z^2}$-AOs of copper(II) [33, 34].

Comparative analysis of the EPR parameters (Table 1) shows that the solvation often has opposing effects on A_1^{Cu} and A_2^{Cu}: the former decreases, while the latter increases [17, 18, 22, 35]. The difference between the constants A_1^{Cu} and A_2^{Cu} (the parameter Δ) serves as a quantitative estimate of the TBP contribution to the geometry of the copper polyhedron. There has been revealed an inverse relationship: the smaller the parameter Δ, the more considerable the TBP contribution. For complex **II**, Δ decreases to 66 G against the nonsolvated isomeric forms (Δ = 114 and 112 G). Therefore, the solvation of the starting adduct $[^{63}Cu\{NH(CH_2)_4O\}\{S_2CN(C_2H_5)_2\}_2]$ causes its two molecular forms to change into a new state characterized by a greater TBP contribution to the geometry of the coordination polyhedron of copper. Since in the study of the diamagnetic complex $[Zn\{NH(CH_2)_4O\}\{S_2CN(C_2H_5)_2\}_2] \cdot CCl_4$, copper(II) served as a spin probe more or less accurately reflecting the structural features of the matrix, we found it interesting to examine complex **I** by solid-state NMR MAS spectroscopy.

The ^{13}C MAS NMR spectrum (Fig. 2) of a polycrystalline sample of **I** shows sets of signals for the diethyldithiocarbamate ligands, the coordinated morpholine molecules, and the "guest" molecules of CCl_4 (Table 2). Based on the experimental values of the ^{13}C chemical shifts for $Na\{S_2CN(C_2H_5)_2\} \cdot 3H_2O$, one can identify the signals for the CH_3-, $-CH_2-$, and $=NC(S)S-$ groups; the morpholine ligand is manifested as signals for the carbon atoms in the $-OCH_2-$ and $=NCH_2-$ fragments [17]. In contrast to the nonsolvated adduct [18], the solvation with CCl_4 complicates the spectral pattern in the ranges characteristic of both Edtc and morpholine ligands (a triplet and a doublet appear for the $-OCH_2-$ and $=NCH_2-$ fragments, respectively). Four resonance signals at δ 202.2, 202.8, 203.2, and 203.7 with relative intensities of ~1 : 1 : 1 : 1 are all due to the dithiocarbamate groups, thus confirming the presence of two types of

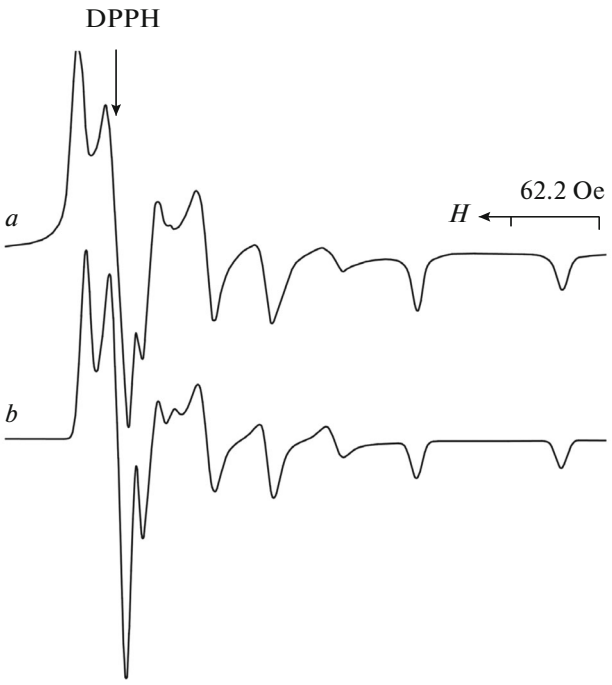

Fig. 1. Experimental (*a*) and simulated EPR spectra (*b*) of magnetically diluted complex **II**.

structurally nonequivalent molecules in the adduct (Fig. 2, Table 2).

A pair of signals at δ 96.9 and 97.2 for the outer-sphere CCl_4 molecule also provides evidence for the presence of two structurally nonequivalent "guest" molecules in the crystal lattice. Interestingly, the ^{13}C MAS NMR spectra of the solvate systems studied in [15, 17, 18, 20–22, 37, 38] always contained a single resonance signal for their outer-sphere molecules. The ^{13}C chemical shifts for the CCl_4 molecules in the solvated adduct are somewhat larger than those for CCl_4 as an individual solvent [36], which is due to their interactions with the crystal lattice of $[Zn\{NH(CH_2)_4O\}\{S_2CN(C_2H_5)_2\}_2]$.

The unit cell of supramolecular complex **I** comprises four formula units; each unit consists of an adduct molecule and an outer-sphere solvate molecule of CCl_4 (Fig. 3). The noncentrosymmetric complex under discussion contains two structurally non-

Table 1. Parameters of the EPR spectrum of complex **II**

Complex	g_1	A_1^{Cu}*	g_2	A_1^{Cu}*	g_3	A_3 *
II	2.123	120	2.066	54	2.017	15
[17]**	2.121	135/145	2.038	21/23	2.038	21/23
	2.120	133/143	2.038	21/23	2.038	21/23

* The hyperfine constants are given for $^{63}Cu/^{65}Cu$.
** The data for two isomers of the adduct.

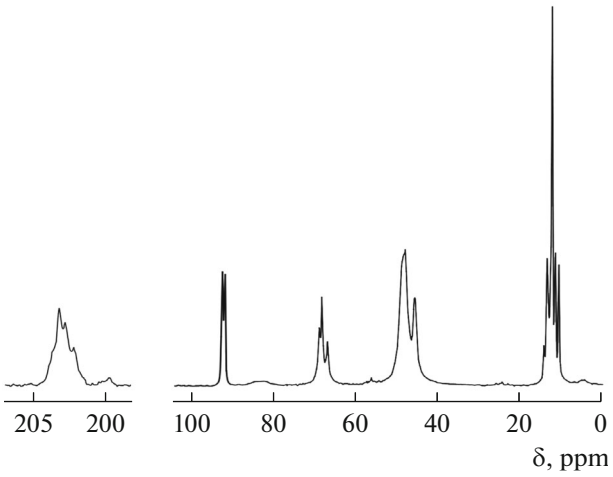

Fig. 2. ^{13}C MAS NMR spectrum of adduct **I**. The number of transients/spinning rate are 14400/4500 Hz.

equivalent molecules A and B of the adduct and two structurally nonequivalent outer-sphere CCl_4 molecules (Table 3). This complex is mainly stabilized by weak hydrogen bonds between the morpholine rings and by short intermolecular contacts involving the Cl atoms of the solvate CCl_4 molecules, the S atoms of the Edtc ligands, and the morpholine O atoms (Table 3).

In adducts A and B, the zinc atoms are coordinated by two dithiocarbamate ligands in an S,S'-bidentate fashion and by a morpholine molecule in an N-monodentate fashion, so their coordination environment is $[S_4N]$ (C.N. 5) (Fig. 3). Despite considerable similarity, they are structurally nonequivalent (hereafter, Zn(1) refers to molecule A and Zn(2), to B). Let us consider the most substantial structural differences between molecules A and B.

All the ligands feature anisobidentate coordination: one Zn–S bond (A: 2.316 and 2.335 Å; B: 2.323 and 2.338 Å) is appreciably stronger than the other (A: 2.541 and 2.685 Å; B: 2.522 and 2.659 Å) (Table 3). This type of coordination of the =NC(S)S– groups gives rise to small four-membered chelate rings $[ZnS_2C]$ characterized by very short Zn···C (A: 2.836 and 2.910 Å; B: 2.824 and 2.888 Å) and S···S distances (A: 2.936 and 2.954 Å; B: 2.946 and 2.951 Å). The planar geometry of the chelate rings shows a tetrahedral distortion due to the folding of the ring along the S–S axis. In adduct B, neither chelate ring is planar. The torsion angles CSSZn and SZnCS are 172.50°, 175.09° and 173.78°, 175.90°, respectively. In adduct A, the C(10)-containing ring is distorted (173.43° and

Table 2. Chemical shifts δ (ppm) in the ^{13}C NMR spectrum of complex **I**

$-S(S)CN(C_2H_5)_2$			$O(CH_2)_4NH$		$CCl_4/CHCl_3$	Reference
$=NCS_2-$	$-CH_2-$	$-CH_3$	$-O-CH_2-$	$=N-CH_2-$		
205.8	49.7	14.5	67.8	51.2		[18]
204.5		13.4				
203.9		12.6				
		12.3				
203.7	49.11	14.7	69.8	48.6	97.2	This study
203.2		13.9	69.1	46.3	96.9	
202.8		13.8	67.8			
202.2		13.4				
		12.7				
		11.9				
		10.9				
202.8	49.3	13.2	69.0	47.3	80.9	[22]
202.3	49.0	12.9	68.5			
		12.5				
		11.6				
					77.2	[36] ($CHCl_3$)
					96.0	[36] (CCl_4)

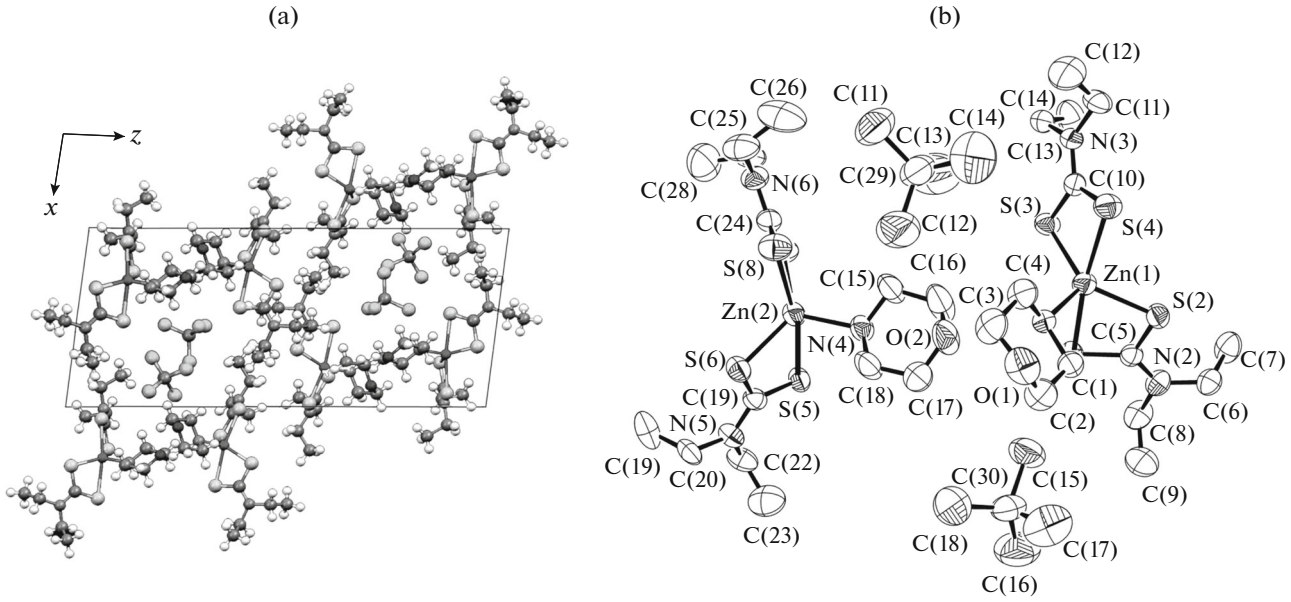

Fig. 3. Projection of the crystal structure of complex **I** onto the plane *xz* (a) and a fragment of its molecular structure (b).

174.51°), while the C(5)-containing ring is nearly planar (178.94° and 179.10°).

Because of the mesomeric effect in the dithiocarbamate groups, the N–C(S)S bond (1.309–1.339 Å) is noticeably shorter than the N–C_2H_5 bond (1.446–1.501 Å) (Table 3), which reflects a considerable contribution of double bonding to the formally single bond as well as the mixing of the sp^2- with sp^3-hybridization state of the N and C atoms in the =NC(S)S– groups.

The direct consequence of the solvation of the starting adduct is that the TP geometry of the zinc polyhedron is substantially TBP-distorted. Zinc polyhedra [$ZnNS_4$] are intermediate between TP and TBP. The metal polyhedra in five-coordinate complexes are conveniently described using the quantitative parameter $\tau = (\alpha - \beta)/60$ [39] ($\alpha > \beta$ are the largest two LZnL angles). In a regular TP (C_{4v}), $\tau = 0$ because of $\alpha = \beta$. In a regular TBP (C_{3v}), the axial angle α is 180° (LZnL), while the equatorial angle β is 120° (so $\tau = 1$). For intermediate polyhedra, τ ranges from 0 to 1. In adduct A, the angle S(1)Zn(1)S(4) (α) is 166.99° and the angle S(2)Zn(1)S(3) (β) is 126.86° ($\tau = 0.67$). In B, the angle S(5)Zn(2)S(7) (α) is 171.07° and the angle S(6)Zn(1)S(8) (β) is 127.08° ($\tau = 0.73$). Therefore, the TBP contribution in adduct B is more considerable (73%) than that in A (67%) (for the nonsolvated adduct, this contribution is ~4% [18]). The equatorial plane of the TBP is made up of the N atom of morpholine and two most strongly bound S atoms (A: N(1), S(2), and S(3); B: N(4), S(6), and S(8)). The less strongly bound atoms (S(1), S(4), S(5), and S(7)) are in axial positions (Fig. 3).

The isomeric solvate molecules of CCl_4 in the crystal lattice are stabilized by short contacts between the Cl atoms and the S atoms of the Edtc ligands: Cl(1)···S(5)^{ii}, 3.245 Å; Cl(5)···S(1), 3.297 Å; Cl(8)···S(5)^{ii}, 3.466 Å (these are all somewhat shorter than the sum of the van der Waals radii of the Cl and S atoms (3.55 Å) [40–42]) and between the Cl atom and the morpholine O atom (Cl(3)···O(1)^{i}, 3.245 Å). Such contacts involving highly polarized atoms differ from hydrogen bonding and π-stacking and are due to interactions between induced dipoles in the crystal.

The thermolysis of complex **I** involves the following sequential steps: removal of the solvate CCl_4 molecules from the crystal lattice, desorption of the chemically bound morpholine molecules, and degradation of the dithiocarbamate complex (Fig. 4). According to the TG data, the CCl_4 molecules desorb below 100.0°C with a weight loss of 25.11% (the calculated value is 25.55%). The endothermic effect on the DSC curve with a minimum at 67.7°C corresponds to the melting of the sample (T_m = 65°C was measured independently in a glass capillary). Between 100 and 216°C, the Zn–N bonds dissociate to eliminate the morpholine molecules; the weight loss is 13.18% (the calculated value is 14.43%). The final step occurs in a temperature range between 216 and 340°C. This step is commonly due to the thermolysis of the "dithiocarbamate moiety" of the zinc complex to ZnS. The DSC curve shows the corresponding endothermic effect with a minimum at 330.5°C (thermal degradation and evaporation). The residual weight of the sample was 6.83%, which is lower by a factor of 2.5 than the calculated value (17.16%). Such volatility of the complex

Table 3. Selected bond lengths *d* and bond angles ω in structure **I***

Adduct A		Adduct B	
Bond	*d*, Å	Bond	*d*, Å
Zn(1)–N(1)	2.084(7)	Zn(2)–N(4)	2.078(8)
Zn(1)–S(1)	2.685(3)	Zn(2)–S(5)	2.659(3)
Zn(1)–S(2)	2.316(3)	Zn(2)–S(6)	2.323(3)
Zn(1)–S(3)	2.335(3)	Zn(2)–S(7)	2.522(3)
Zn(1)–S(4)	2.541(3)	Zn(2)–S(8)	2.338(3)
S(1)–C(5)	1.719(9)	S(5)–C(19)	1.705(1)
S(2)–C(5)	1.731(9)	S(6)–C(19)	1.732(1)
S(3)–C(10)	1.718(9)	S(7)–C(24)	1.707(1)
S(4)–C(10)	1.719(9)	S(8)–C(24)	1.740(1)
N(2)–C(5)	1.330(1)	N(5)–C(19)	1.339(1)
N(3)–C(10)	1.322(1)	N(6)–C(24)	1.309(1)
N(2)–C(6)	1.481(1)	N(5)–C(20)	1.501(1)
N(2)–C(8)	1.484(1)	N(5)–C(22)	1.446(1)
Angle	ω, deg	Angle	ω, deg
Zn(1)N(1)C(1)	111.8(5)	Zn(2)N(4)C(15)	116.1(7)
Zn(1)N(1)C(4)	117.9(6)	Zn(2)N(4)C(18)	114.6(7)
N(1)Zn(1)S(1)	89.8(2)	N(4)Zn(2)S(5)	88.0(2)
N(1)Zn(1)S(2)	114.6(2)	N(4)Zn(2)S(6)	116.5(3)
N(1)Zn(1)S(3)	118.0(2)	N(4)Zn(2)S(7)	100.9(2)
N(1)Zn(1)S(4)	103.2(2)	N(4)Zn(2)S(8)	115.8(3)
Zn(1)S(1)C(5)	79.4(3)	Zn(2)S(5)C(19)	79.6(3)
Zn(1)S(2)C(5)	90.8(3)	Zn(2)S(6)C(19)	89.6(3)
Zn(1)S(3)C(10)	87.4(3)	Zn(2)S(7)C(24)	81.3(3)
Zn(1)S(4)C(10)	81.0(3)	Zn(2)S(8)C(24)	86.3(4)
S(1)Zn(1)S(2)	71.99(8)	S(5)Zn(2)S(6)	72.29(9)
S(3)Zn(1)S(4)	73.91(8)	S(7)Zn(2)S(8)	74.50(1)
S(1)Zn(1)S(3)	100.67(9)	S(5)Zn(2)S(7)	171.07(1)
S(1)Zn(1)S(4)	166.99(9)	S(5)Zn(2)S(8)	102.40(1)
S(2)Zn(1)S(3)	126.86(1)	S(6)Zn(2)S(7)	102.65(1)
S(2)Zn(1)S(4)	101.47(9)	S(6)Zn(2)S(8)	127.08(1)
Short intermolecular contacts, Å			
Cl(1)···S(5)^{ii}	3.245(6)	Cl(5)···S(1)	3.297(5)
Cl(3)···O(1)^{i}	3.168(12)		
Intermolecular hydrogen bonds, Å			
D–H···A	D–H	H···A	D···A	D··H···A
N(1)–H(1)···O(2)	0.91	2.21	3.077(12)	159

* The symmetry operations: ^{i} x, $1+y$, z; ^{ii} $1+x$, y, z.

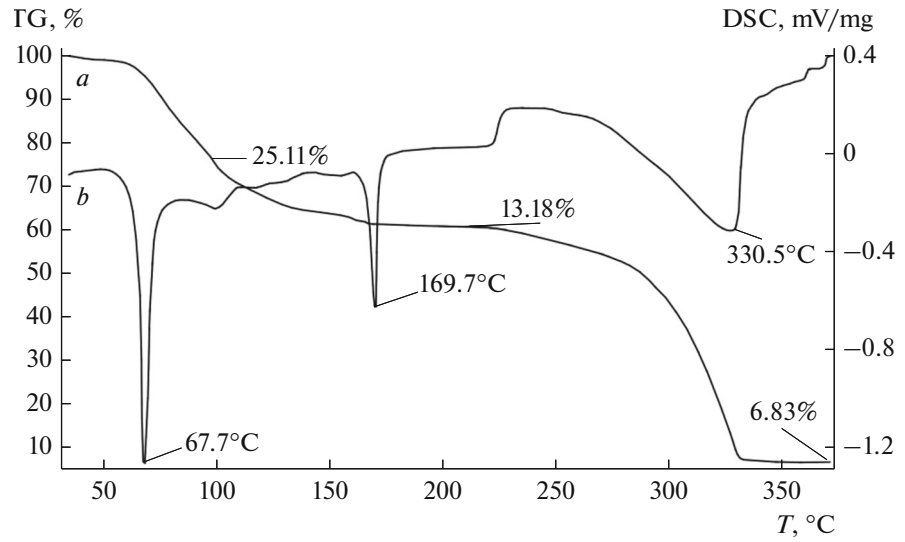

Fig. 4. TG (*a*) and DSC curves (*b*) for adduct **I**.

under the thermolysis conditions (dynamic argon atmosphere) has been reported earlier [22, 43].

We are grateful to O.N. Antsutkin (Luleå University of Technology, Luleå, Sweden) for his assistance in the MAS NMR experiments and to Bruker Co. for free access to the WIN-EPR SimFonia program.

REFERENCES

1. Decken, A., Gossage, R.A., Chan, M.Y., et al., *Appl. Organomet. Chem.*, 2004, vol. 18, no. 2, p. 101.
2. Siddiqi, K.S., Nami, S.A.A., and Chebude Lutfullah, Y., *J. Braz. Chem. Soc.*, 2006, vol. 17, no. 1, p. 107.
3. Khan, S., Nami, S.A.A., and Siddiqi, K.S., *J. Mol. Struct.*, 2008, vol. 875, nos. 1–3, p. 478.
4. Prakasam, B.A., Ramalingam, K., Bocelli, G., and Cantoni, A., *Polyhedron*, 2007, vol. 26, no. 15, p. 4489.
5. Srinivasan, N., Thirumaran, S., and Ciattini, S., *J. Mol. Struct.*, 2009, vol. 936, nos. 1–3, p. 234.
6. Thirumaran, S., Ramalingam, K., Bocelli, G., and Righi, L., *Polyhedron*, 2009, vol. 28, no. 2, p. 263.
7. Srinivasan, N., Sathyaselvabala, V., Kuppulekshmy, K., et al., *Monatsh. Chem.*, 2009, vol. 140, no. 12, p. 1431.
8. Subha, P.V., Valarmathi, P., Srinivasan, N., et al., *Polyhedron*, 2010, vol. 29, no. 3, p. 1078.
9. Onwudiwe, D.C. and Ajibade, P.A., *Polyhedron*, 2010, vol. 29, no. 5, p. 1431.
10. Mamba, S.M., Mishra, A.K., Mamba, B.B., et al., *Spectrochim. Acta, Part A*, 2010, vol. 77, no. 3, p. 579.
11. Mishra, A.K. and Kaushik, N.K., *Spectrochim. Acta., Part. A*, 2008, vol. 69, no. 3, p. 842.
12. Ajibade, P.A., Onwudiwe, D.C., and Moloto, M.J., *Polyhedron*, 2011, vol. 30, no. 2, p. 246.
13. Marx, N.R., Pandian, K., and Sivakumar, K., *Appl. Surf. Sci.*, 2011, vol. 257, no. 7, p. 2745.
14. Dulare, R., Bharty, M.K., Singh, A., and Singh, N.K., *Polyhedron*, 2012, vol. 31, no. 1, p. 373.
15. Ivanov, A.V., Leskova, S.A., Mel'nikova, M.A., et al., *Russ. J. Inorg. Chem.*, 2003, vol. 48, no. 3, p. 415.
16. O'Brien, P., in *Inorganic Materials*, Bruce, D.W. and Hare, D., Eds., New York: Wiley, 1992, p. 500
17. Ivanov, A.V., Forshling, V., Kritikos, M., et al., *Dokl. Ross. Akad. Nauk*, 1999, vol. 369, no. 1, p. 64.
18. Ivanov, A.V., Kritikos, M., Antzutkin, O.N., and Forsling, W., *Inorg. Chim. Acta*, 2001, vol. 321, nos. 1–2, p. 63.
19. Ivanov, A.V. and Antzutkin, O.N., *Top. Curr. Chem.*, 2005, vol. 246, p. 271.
20. Ivanov, A.V., Lutsenko, I.A., Gerasimenko, A.V., and Merkulov, E.B., *Russ. J. Inorg. Chem.*, 2008, vol. 53, no. 2, p. 293.
21. Ivanov, A.V., Lutsenko, I.A., Zaeva, A.S., et al., *Russ. J. Coord. Chem.*, 2007, vol. 33, no. 11, p. 815.
22. Lutsenko, I.A., Ivanov, A.V., Korneeva, E.V., and Tursina, A.I., *Russ. J. Coord. Chem.*, 2012, vol. 38, no. 11, p. 709.
23. Bonamico, M., Mazzone, G., Vaciago, A., and Zambonelli, L., *Acta Crystallogr.*, 1965, vol. 19, no. 6, p. 898.
24. Bennett, A.E., Rienstra, C.M., Auger, M., et al., *J. Chem. Phys.*, 1995, vol. 103, no. 13, p. 6951.
25. Earl, W.L. and Vanderhart, D.L., *J. Magn. Reson.*, 1982, vol. 48, no. 1, p. 35.
26. Morcombe, C.R. and Zilm, K.W., *J. Magn. Reson.*, 2003, vol. 162, no. 2, p. 479.
27. Farrugia, L.J., *J. Appl. Crystallogr.*, 1999, vol. 32, no. 4, p. 837.
28. North, A.C.T., Phillips, D.C., and Mathews, F.S., *Acta Crystallogr., Sect. A: Cryst. Phys., Diffr., Theor. Gen. Crystallogr.,* 1968, vol. 64, no. 3, p 351.
29. Sheldrick, G.M., *Acta Crystallogr., Sect. A: Found. Crystallogr.*, 2008, vol. 64, no. 1, p. 112.

30. Flack, H.D., *Acta Crystallogr., Sect. A: Found. Crystallogr.*, 1983, vol. 39, no. 6, p. 876.
31. Rieger, Ph.H., *Electron Spin Resonance*, Athenaeum, 1993, vol. 13B, p. 178.
32. Ovchinnikov, I.V. and Konstantinov, V.N., *J. Magn. Reson.*, 1978, vol. 32, no. 2, p. 179.
33. Arriortua, M.A., Mesa, J.L., Rojo, T., et al., *Inorg. Chem.*, 1988, vol. 27, no. 17, p. 2976.
34. Murakami, T., Takei, T., and Ishikawa, Y., *Polyhedron*, 1997, vol. 16, no. 1, p. 89.
35. Ivanov, A.V., Forshling, V., Antsutkin, O.N., and Novikova, E.V., *Russ. J. Coord. Chem.*, 2001, vol. 27, no. 3, p. 158.
36. Levy, G.C., Lichter, R.L., and Nelson, G.L., *Carbon-13 Nuclear Magnetic Resonance Spectroscopy*, New York: Wiley, 1980.
37. Ivanov, A.V., Forshling, V., Antsutkin, O.N., et al., *Dokl. Ross. Akad. Nauk*, 1999, vol. 366, no. 5, p. 643.
38. Ivanov, A.V., Lutsenko, I.A., and Forshling, V., *Russ. J. Coord. Chem.*, 2002, vol. 28, no. 1, p. 57.
39. Addison, A.W., Rao, T.N., Reedijk, J., et al., *J. Chem. Soc., Dalton Trans.*, 1984, no. 7, p. 1349.
40. Pauling, L., *The Nature of the Chemical Bond and the Structure of Molecules and Crystals*, London: Cornell Univ., 1960.
41. Bondi, A., *J. Phys. Chem.*, 1964, vol. 68, no. 3, p. 441.
42. Bondi, A., *J. Phys. Chem.*, 1966, vol. 70, no. 9, p. 3006.
43. Tavlaridis, A. and Neeb, R., *Fresenius' Z. Anal. Chem.*, 1978, vol. 293, p. 211.

Translated by D. Tolkachev